The University of Auckland
Department of Engineering Science

Part IV Project

Data-Worth Analysis for Geophysical Problems

Author:
Henry Alferink

Supervisors:
Dr Oliver J. Maclaren
Dr Ru Nicholson

April 20, 2021

Acknowledgements

This paper includes citations for direct references. However, because I am not citing the following, I would additionally like to acknowledge that much of the knowledge and ideas in this paper resulted from:

- My supervisors Dr Oliver J. Maclaren and Dr Ru Nicholson.
- My participation in the course MATHS 766 at The University of Auckland in 2020. This course was taught by Dr Marie Graff and Professor Jari Kaipio.

In addition, while it is cited in this paper, I would like to acknowledge the particular usefulness of the book *Parameter Estimation and Inverse Problems* by R. C. Aster, B. Borchers, and C. H. Thurbur.

Contents

1 Introduction **3**

1.1 Introduction to Inverse Problems 3

1.1.1 What is an Inverse Problem? 3

1.1.2 A Simple Example in the Frequentist Framework 5

2 Methodology **7**

2.1 The Bayesian Framework for Inverse Problems 7

2.1.1 Introduction to the Bayesian Framework 7

2.1.2 Deriving the Likelihood 8

2.1.3 Deriving the Posterior 9

2.2 Data Worth Analysis 11

2.2.1 Linear Algebra Methods for Efficient Computation 12

3 Implementation **14**

3.1 Introduction: Source Reconstruction Example 14

3.2 Mathematical Formulation 14

3.3 Modelling the Noise and Prior 15

3.4 Computational Formulation 18

3.5 Adding Measurements 20

3.6 Dual Objective Data-Worth Analysis 24

Bibliography **30**

1 Introduction

A mathematical model often simulates a real world system. Therefore we have two ways to get the data associated with this system: we either gather the data *by hand* with measurement equipment, or we simulate the data with the mathematical model. These mathematical models usually contain parameters that require calibration so that model outputs produce results consistent with reality. In simple terms, this process of calibration is carried out through a process of choosing model parameters such that the model output lines up with real world data.

As mentioned, real world data is used to calibrate mathematical models. However, not all data is equally useful for this purpose. The usefulness of data can be characterized by how efficiently it calibrates the model, or how much it reduces the uncertainty in the model's output. *Data-worth analysis* (also called *optimal experimental design*, or *decision analysis*), which is the topic of this paper, asks the question, "given we have many locations to gather data, which locations give us the most useful data?" This question becomes particularly important when dealing with data that costs a lot to acquire. In order to calibrate a mathematical model we often need to solve an inverse problem. In this paper we define what inverse problems are, and show how we can solve them in practice.

The goal of this paper is to show that data-worth analysis can be used in a geophysical setting, and to provide a methodology in the case of either a linear or non-linear forward problem. We show this methodology by working through a linear example: the source reconstruction problem. However, we also provide the framework to work in a non-linear setting. The main question of data-worth analysis is to ask which data reduces the uncertainty in our solution the most. However, in this paper we additionally look at the case where the data we want to gather is expensive. We therefore need to consider a multi-objective function of reducing both uncertainty as well as cost of measurement.

Some of the work of this project has been put into a conference paper for the New Zealand Geothermal Workshop (NZGW) [1].

1.1 Introduction to Inverse Problems

1.1.1 What is an Inverse Problem?

To describe what an inverse problem is, we will begin by describing a forward problem. A forward problem is the typical mathematical formulation we are all used to: we have some mathematical model $g : \mathbb{R}^n \to \mathbb{R}^m$ (also called a *forward operator*), a set of parameters $x \in \mathbb{R}^n$ to plug into that model, and seek the resulting model output $d_{model} \in \mathbb{R}^m$ (this is

the so-called *data* that the model produces). In other words,

$$d_{model} = g(x).$$

Forward problems come in many different forms, and could take from an arbitrarily small time to compute, to sometimes taking weeks to compute. Note that the focus of this project is not on formulating the forward problem. We assume it is known.

On the other hand, if we have a forward operator which models a physical process; and if we have collected real world data corresponding to that process; then we might ask the question, "Which parameters should I input into the model such that my collected data would be reproduced?" This is the inverse problem, and in its most basic form is expressed as

$$x = g^{-1}(d_{model}).$$

However, since we are dealing with real world data that contains noise, the forward problem becomes

$$d = d_{model} + \varepsilon$$

where ε is a random variable that models the noise. This is the *additive error* case. There are also other possible error models, such as multiplicative error. In this project, however, we assume the additive error model and that ε is normally distributed. From hereon we refer to d as the *data vector.*

There are three main issues that come up when dealing with inverse problems. If the problem exhibits any of these issues we say that it is *ill-posed*. The field of inverse problems seeks to find solutions to all of these.

1. **Non-Existence:** where there is no exact solution to the system. Often this is due to the noise term, which (in in the linear sense) takes the data outside of the column space of the forward operator. As we will see shortly, this issue is solved by using the least squares estimate, which projects the data vector onto the column space, thus making the inverse problem solvable.

2. **Non-Uniqueness:** where there are multiple (usually infinite) possible solutions to the system. This begs the question, which solution do we choose? A basic example of this is the equation $f(x) = x^2$. The inverse of $f(x)$ has two solutions for all $x \neq 0$. The way to solve this issue lies in constraining the solution set somehow. We outline a few methods of constraining the solution set in this paper.

3. **Instability:** where a small change in the data vector causes a large change in the parameter solution (in the inverse problem). This means that even relatively small perturbations of noise in the data can cause vastly different results for the parameter solution.

1.1.2 A Simple Example in the Frequentist Framework

A simple example is a projectile motion problem: here we have noisy data that captures the height a projectile reaches at certain points in time, and seek to fit a continuous function to this data. Although the parameters are unknown to us, we assume they are fixed; this is the foundational assumption of the ferequentist framework. Opposed to this is the Bayesian framework (which we will see more of later), which assumes the parameters themselves are random variables, i.e. not necessarily fixed. A mathematical model that characterizes projectile motion is expressed in the following function:

$$d_{model}(t) = x_1 + x_2 t - \frac{1}{2} x_3 t^2.$$

Here we still need to determine the parameters $x = \begin{bmatrix} x_1 & x_2 & x_3 \end{bmatrix}^T$ that cause the function to best fit the given data. The function is linear in its parameters, so, recalling that d refers to the noisy data (i.e. it includes the normally distributed noise term), the forward problem can be expressed as

$$d = Gx + \varepsilon,$$

i.e.,

$$\begin{bmatrix} d(t_1) \\ d(t_2) \\ \vdots \\ d(t_m) \end{bmatrix} = \begin{bmatrix} 1 & t_1 & -\frac{1}{2}t_1^2 \\ 1 & t_2 & -\frac{1}{2}t_2^2 \\ \vdots & & \\ 1 & t_m & -\frac{1}{2}t_m^2 \end{bmatrix} \begin{bmatrix} x_1 \\ x_2 \\ x_3 \end{bmatrix} + \begin{bmatrix} \varepsilon_1 \\ \varepsilon_2 \\ \vdots \\ \varepsilon_m \end{bmatrix}.$$

Finding the correct parameters is a minimization problem. We need to minimize the residual (defined as the difference between the empirical data and the model output) subject to some norm (which we will always take as the 2-norm in this paper):

$$x_{LS} = \underset{x}{\operatorname{argmin}} \, ||d - d_{model}||_2^2 \,, \tag{1.1}$$

where x_{LS} is the solution of the inverse problem in the least-squares sense. If $G^T G$ is invertible, we can use the *normal equations* to find the solution:

$$x_{LS} = (G^T G)^{-1} G^T d.$$

The black line in figure 1 shows the true motion of the projectile. The empirical datapoints are shown as black points. For example purposes these are simply the true motion plus some normally distributed noise. Note that the true motion will be unknown in reality. In reality we only have access to the measurement data, which will always contain some level of noise. The least squares estimate of the true motion is the matrix multiplication Gx_{LS}. Figure 1 shows that in this example the least squares estimate is clearly a good approximation. When we have an *overdetermined* system this is often the case. An overdetermined system is where we have more data points than the number of parameters we are trying to estimate

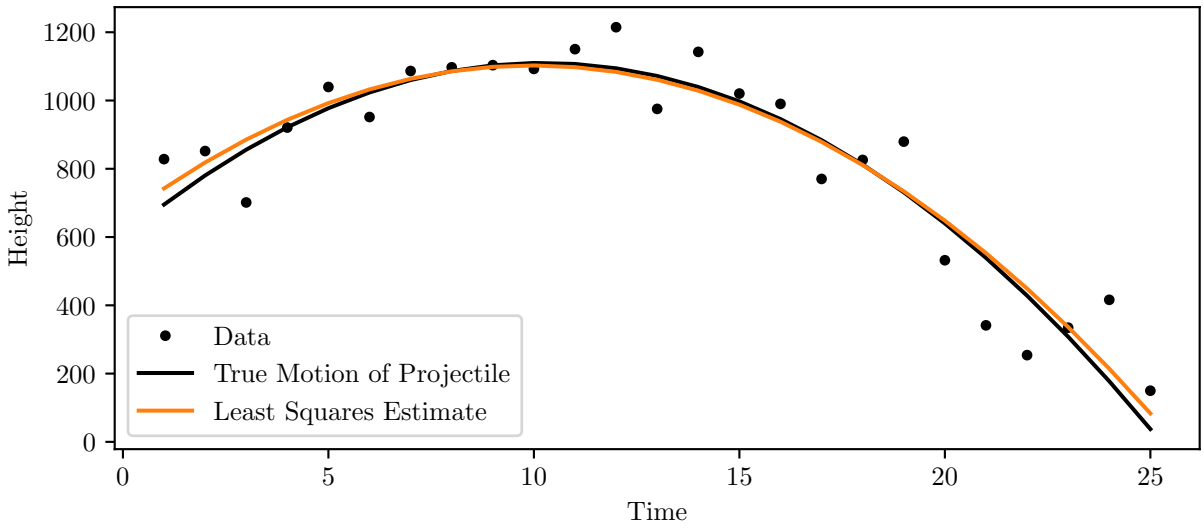

Figure 1: Projectile motion example. The data points shown are taken from the true model with some normally distributed noise added.

(i.e. $m > n$). Moreover, an over-determined system usually results in a unique solution. However, when the system is *underdetermined* we will always be faced with the issue of non-uniqueness. This is because, when $m < n$, the null space of the forward operator G will be non-trivial, and hence there will exist an infinite number of solutions. Moreover, when the null space of G is non-trivial, the inverse of $G^T G$ does not exist and so we cannot use the normal equations.

A simple way in which we can always find the solution to the underdetermined case is to use the pseudo-inverse $G^\dagger$. The pseudo-inverse solution is found by taking $x_\dagger = G^\dagger d$. This is still a least-squares method and works in a similar way to the normal equations, but the problem of having an infinite number of solutions is overcome by choosing the one with the minimum norm (the *smallest one*, in overly-simplistic terms). $x_\dagger$ is therefore called the *minimum norm solution*. However, due to the ill-posed nature of many inverse problems, the minimum norm solution is often not ideal, and regularization methods such as Tikhonov regularisation or the truncated SVD (singular value decomposition) method should be used. In the case of Tikhonov regularization, the following functional is used instead of (1.1):

$$x_{Tik} = \underset{x}{\operatorname{argmin}} \, ||d - Gx||_2^2 + \alpha \, ||x||_2^2 \,,$$

where $\alpha > 0$ is a tuning parameter. From this expression we can see that x_{Tik} seeks a good trade-off between the size of the residual and the size of the model. Computationally, we can find the Tikhonov solution by evaluating

$$x_{Tik} = (G^T G + \alpha I)^{-1} G^T d.$$

2 Methodology

2.1 The Bayesian Framework for Inverse Problems

2.1.1 Introduction to the Bayesian Framework

The analysis used in the introduction was done in the *frequentist* statistical framework. This framework assumes the parameter solution x is an unknown but fixed value we are trying to find. We then estimate this fixed value by evaluating some function of the data. Moreover, we saw that in the frequentist view, a Tikhonov regularized solution can be found to give a good estimate for an underdetermined inverse problem. However, there are problems with the frequentist framework. In particular, in the case of data-worth analysis, it does not allow for straight forward uncertainty quantification.

Instead of using the frequentist view of the parameters, we can use the *Bayesian* framework. This is the framework we use from hereon. The Bayesian framework no longer assumes the parameter x is fixed, but assumes it is a random variable with a probability distribution. The expectation of this distribution is then a value we commonly use to represent the parameter solution. One advantage of using the Bayesian framework in the context of data-worth analysis is that it naturally allows us to model the *uncertainty* in the data and parameters. This is important because we want to find a relationship between the uncertainty in the data and the uncertainty in the parameters so that we can analyze how to reduce parameter uncertainty as much as possible.

Baye's rule is stated as

$$\pi(x|d) = \frac{\pi(d|x)\pi(x)}{\pi(d)}.$$

However, the denominator is a constant and is not of much use to us, so we simplify Baye's rule to

$$\pi(x|d) \propto \pi(d|x)\pi(x).$$

Each term in Baye's formula is a probability distribution. The $\pi(d|x)$ term is called the *likelihood* and models the measurement process, i.e. the noise in the data. $\pi(x)$ is called the *prior* and is used to encode our prior belief about the parameters. The prior can be seen as taking a similar role to what regularization does in the frequentist framework. Note that if we do not have any prior knowledge about the parameters, it is possible to use an *uninformative prior* which is essentially a flat distribution that holds little to no information. However, it is often beneficial to use a prior. For example, it is possible to encode in the prior the belief that our parameters will produce a relatively smooth function as opposed to a choppy one.

The $\pi(x|d)$ term is called the *posterior*. In practical terms, this is our parameter solution in

the Bayesian framework. As mentioned, this is a probability distribution from which we can take an expected value, credible intervals (similar to the frequentist notion of a *confidence interval*), etc.

2.1.2 Deriving the Likelihood

To derive the likelihood we start by restating the measurement equation:

$$d = g(x) + \varepsilon.$$

This equation contains three random variables: d, x, and e. For our project we utilize the common assumption that x is independent of the measurement errors e. This assumption makes calculations simpler. It is possible, however, to derive the likelihood for dependent x and e. Furthermore, it is also possible to derive the likelihood for other measurement models such as multiplicative error. In our case, the joint density can be expressed as both

$$\pi(d, x, e) = \pi(d|x, e)\pi(x)\pi(e) \quad \text{and} \quad \pi(d, x, e) = \pi(d, e|x)\pi(x).$$

Putting these together we get

$$\pi(d, e|x) = \pi(d|x, e)\pi(e).$$

We can now marginalize to get rid of the e variable:

$$\pi(d|x) = \int_{-\infty}^{\infty} \pi(d|x, e)\pi(e)de = \int_{-\infty}^{\infty} \delta(e - (d - g(x)))\pi(e)de.$$

Here $\pi(d|x, e)$ gets replaced by a delta distribution because d is fully determined (because when the random variables x and e are known, d is also known exactly). Since the delta distribution has the following property (for some function φ):

$$\int_{-\infty}^{\infty} \varphi(t)\delta(t - t_0)dt = \varphi(t_0),$$

we have

$$\pi(d|x) = \pi_e(d - g(x)).$$

In other words, to derive the likelihood for the additive error case where x and e are independent, we just need to know the probability density for the error term evaluated at $d - g(x)$.

2.1.3 Deriving the Posterior

Here we show how to find the posterior distribution. Once we have the posterior we can then take the posterior mean and covariance matrix, the latter being of key importance in data-worth analysis. In this project we assume that the error term is normally distributed with 0 mean and we also use a normal distribution for the prior. We denote the covariance matrices of the error and the prior as Γ_e and Γ_x respectively, and the mean of the prior as μ_x. Furthermore, we also take the Cholesky decomposition of the covariance matrix inverses: $\Gamma_e^{-1} = L_e^T L_e$, and $\Gamma_x^{-1} = L_x^T L_x$. The posterior is therefore given by,

$$\begin{aligned}
\pi(x|d) \propto \pi(d|x)\pi(x) &= \pi_e(d - g(x))\pi(x) \\
&= \exp\left\{-\frac{1}{2}(d-g(x))^T\Gamma_e^{-1}(d-g(x))\right\}\exp\left\{-\frac{1}{2}(x-\mu_x)^T\Gamma_x^{-1}(x-\mu_x)\right\} \\
&= \exp\left\{-\frac{1}{2}\Big((d-g(x))^T\Gamma_e^{-1}(d-g(x)) + (x-\mu_x)^T\Gamma_x^{-1}(x-\mu_x)\Big)\right\} \\
&= \exp\left\{-\frac{1}{2}\Big((d-g(x))^T L_e^T L_e(d-g(x)) + (x-\mu_x)^T L_x^T L_x(x-\mu_x)\Big)\right\} \\
&= \exp\left\{-\frac{1}{2}\Big(\,||L_e(d-g(x))||_2^2 + ||L_x(x-\mu_x)||_2^2\,\Big)\right\} \qquad (2.1)
\end{aligned}$$

Non-Linear Forward Operator

In the case of a non-linear forward operator, the posterior is generally not a normal distribution. In this case we could use the Markov Chain Monte Carlo (MCMC) method to obtain the posterior distribution, however this can prove to be intractable if the forward operator takes a long time to run. A simple way to overcome this is to approximate the posterior as a normal distribution centered at the *maximum a posteriori* (MAP) point, which is the maximum of the distribution. This is found at the minimizer of the argument to the exponential in (2.1), i.e.,

$$x_{MAP} = \underset{x}{\operatorname{argmin}}\, ||L_e(d-g(x))||_2^2 + ||L_x(x-\mu_x)||_2^2\,.$$

A non-linear optimization method will usually be required to find x_{MAP}. The posterior covariance is found by first linearizing the forward operator:

$$g(x) \approx g(x_{MAP}) + J(x - x_{MAP})$$

where J is the Jacobian matrix of the forward operator evaluated at x_{MAP}. From this it can be shown [2, 3] that the posterior covariance matrix is given by

$$\Gamma_{post} = (J^T\Gamma_e J + \Gamma_x)^{-1}.$$

So, the normally distributed approximation to the posterior is

$$\mathcal{N}(x_{MAP}, \Gamma_{post}).$$

It should be noted that in the non-linear case, the posterior covariance matrix depends on the data vector.

Linear Forward Operator

If the forward operator is linear, we have

$$\pi(x|d) \propto \exp\left\{-\frac{1}{2}\Big((d-Gx)^T\Gamma_e^{-1}(d-Gx) + (x-\mu_x)^T\Gamma_x^{-1}(x-\mu_x)\Big)\right\}.$$

It can be shown [2, 3] that in the linear case the posterior is exactly normal and can be expressed as

$$\pi(x|d) \propto \exp\left\{-\frac{1}{2}\Big((x-x_{MAP})^T\Gamma_{post}^{-1}(x-x_{MAP})\Big)\right\}$$

with

$$x_{MAP} = \mu_x + \Gamma_x G^T(G^T\Gamma_e^{-1}G + \Gamma_x)^{-1}(d - G\mu_x),$$

and

$$\Gamma_{post} = (G^T\Gamma_e^{-1}G + \Gamma_x)^{-1} \tag{2.2}$$

Because the posterior is a normal distribution in this case, the MAP point is also the mean. Note that unlike in the non-linear case, here the posterior covariance matrix does not depend on the data.

Simplifying the above, in practice we evaluate the posterior in the following way. Because each of the norms in (2.1) evaluate to a sum of squared terms, they can be re-expressed as

$$||L_e(d-Gx)||_2^2 + ||L_x(x-\mu_x)||_2^2 = \left|\left|\begin{bmatrix}L_eG\\L_x\end{bmatrix}x - \begin{bmatrix}L_ed\\L_x\mu_x\end{bmatrix}\right|\right|_2^2 = \left|\left|\tilde{G}x - \tilde{d}\right|\right|_2^2,$$

so the posterior can be expressed as

$$\pi(x|d) \propto \exp\left\{-\frac{1}{2}\left|\left|\tilde{G}x - \tilde{d}\right|\right|_2^2\right\}, \quad \tilde{G} = \begin{bmatrix}L_eG\\L_x\end{bmatrix}, \quad \tilde{d} = \begin{bmatrix}L_ed\\L_x\mu_x\end{bmatrix}.$$

This is in the form of a least squares problem, so we can find x_{MAP} by utilizing the normal equations $m_{MAP} = (\tilde{G}^T\tilde{G})^{-1}\tilde{G}^T\tilde{d}$ and Γ_{post} with $\Gamma_{post} = (\tilde{G}^T\tilde{G})^{-1}$ (which just evaluates to (2.2)).

2.2 Data Worth Analysis

Once we have used the analysis described above to get the posterior covariance matrix, we can begin with data-worth analysis. This covariance matrix quantifies the amount of uncertainty in the posterior. We want to choose a measurement scenario such that the covariance matrix is *minimized*. However, to minimize a covariance matrix is in some sense subjective because there are many ways to do this. We need to define an objective function, which we call the uncertainty function, that takes the covariance matrix as input and outputs a single value. A straightforward option called *A-optimality* is simply the average of all the variances, i.e.,

$$\phi_A(\Gamma_{post}) = \frac{1}{n} \operatorname{trace}(\Gamma_{post}).$$

Another option, which takes into account covariances, is *D-optimality*:

$$\phi_D(\Gamma_{post}) = \det(\Gamma_{post}).$$

Note that in practice, if the eigenvalues of Γ_{post} are too small, the second option might not produce useful results. We might in this case want to utilize the sum of the logarithms of the eigenvalues: $\log(\phi_D) = \log(\lambda_1) + \log(\lambda_2) + \cdots + \log(\lambda_n)$. Note that there are of course other possibilities for uncertainty functions such as minimizing only certain subsets of the posterior covariance matrix (see for example [4, 5]).

Another important consideration is whether the problem is posed in a discrete or continuous setting. In other words, are the candidate measurement locations already defined in advance such that we only have a certain number to choose from, or are we essentially free to measure anywhere? In this project we will work only in the discrete case, but see [1] on how to work in a continuous setting.

Furthermore, we might want to take into account the fact that measurements cost different amounts to obtain. We want to avoid high uncertainty and we also want to avoid high cost. We can therefore create a dual objective function that accounts for this:

$$\chi_I = \underset{X \in \mathcal{M}}{\operatorname{argmin}} \, \phi_I(\Gamma_{post}^{(X)}) + P(X).$$

We call the objective function $\phi_I(\Gamma_{post}^{(X)}) + P(X)$ the *total objective*. Recalling that we are working in the discrete setting here, $\mathcal{M}$ is the set containing sets of possible measurement locations. $X \in \mathcal{M}$ is therefore a set containing, e.g., the original measurements that we already had and an additional candidate location. $I \in \{A, D\}$ is the particular uncertainty function we are using; $P(X) \geq 0$ is the cost to obtain the measurement set X; and $\Gamma_{post}^{(X)}$ is the posterior covariance for the measurement set X.

The way in which we carry out the data-worth analysis is as follows:

1. Assuming we already have some data, we evaluate the posterior to obtain the posterior covariance matrix $\Gamma_{post}^{(X_0)}$.

2. Evaluate the objective function $\phi_I(\Gamma_{post}^{(X_0)}) + P(X_0)$.

3. Evaluate an optimization problem that adds measurements (or sets of measurements) X_{new} one at a time to try and minimize $\phi_I(\Gamma_{post}^{(X_0 \cup X_{new})}) + P(X_0 \cup X_{new})$.

We can find $\Gamma_{post}^{(X_0 \cup X_{new})}$ as follows:

$$\Gamma_{post}^{(X_0 \cup X_{new})} = (\widehat{G}^T \widehat{\Gamma}_e^{-1} \widehat{G} + \Gamma_x^{-1})^{-1}, \quad \widehat{G} = \begin{bmatrix} G \\ h \end{bmatrix}, \quad \widehat{\Gamma}_e^{-1} = \begin{bmatrix} \Gamma_e^{-1} & 0 \\ 0 & \sigma_{new}^{-2} \end{bmatrix}$$

where $h \in \mathbb{R}^{1 \times n}$ represents the mapping from the parameters, $x \in \mathbb{R}^n$, to the new measurement. The new measurement is assumed here to have additive noise with standard deviation σ_{new}. In the next section we show a way in which this can be done efficiently. Note that here for simplicity we have only considered the case where one additional measurement has been added, but the case where a set of measurements is added follows trivially.

2.2.1 Linear Algebra Methods for Efficient Computation

Since in the geophysical sphere we are often working with large-scale problems, it is important that we make use of efficient computational techniques. In particular, that we avoid as many matrix inversions as possible. If we already know $\Gamma_{post}^{(X_0)}$, instead of re-evaluating the entire posterior problem to find $\Gamma_{post}^{(X_0 \cup X_{new})}$, we can use the following method. Recalling that $\Gamma_{post}^{-1(X_0)} = G^T \Gamma_e^{-1} G + \Gamma_x^{-1}$ (see (2.2)), where Γ_e and Γ_x are the noise and prior covariances of the measurement set X_0, we can re-write the updated posterior matrix as

$$\begin{aligned} \Gamma_{post}^{(X_0 \cup X_{new})} &= (\widehat{G}^T \widehat{\Gamma}_e^{-1} \widehat{G} + \Gamma_x^{-1})^{-1} \\ &= (G^T \Gamma_e^{-1} G + \Gamma_x^{-1} + \sigma_{new}^{-2} h^T h)^{-1} \\ &= (\Gamma_{post}^{-1(X_0)} + \sigma_{new}^{-2} h^T h)^{-1}. \end{aligned}$$

We can eliminate the need to apply any further matrix inversions by applying the Sherman-Morrison formula:

$$\Gamma_{post}^{(X_0 \cup X_{new})} = \Gamma_{post}^{(X_0)} - \frac{\Gamma_{post}^{(X_0)} h^T h \Gamma_{post}^{(X_0)}}{\sigma_{new}^2 + h \Gamma_{post}^{(X_0)} h^T}.$$

The trace required for ϕ_A is

$$\text{trace}\big(\Gamma_{post}^{(X_0 \cup X_{new})}\big) = \text{trace}\big(\Gamma_{post}^{(X_0)}\big) - \frac{h \Gamma_{post}^{(X_0)} \Gamma_{post}^{(X_0)} h^T}{\sigma_{new}^2 + h \Gamma_{post}^{(X_0)} h^T},$$

and applying the matrix determinant lemma, we get the following which is useful for calculating ϕ_D:

$$\det\left(\Gamma_{post}^{(X_0 \cup X_{new})}\right) = \det\left(\Gamma_{post}^{(X_0)}\right)\left(1 + \frac{h\Gamma_{post}^{(X_0)}h^T}{\sigma_{new}^2 + h\Gamma_{post}^{(X_0)}h^T}\right).$$

3 Implementation

3.1 Introduction: Source Reconstruction Example

In this section we consider a geophysical problem called the *source reconstruction problem*. The main idea was taken from Aster, et al. [6]. We only consider a linear example here, but, as shown in the methodology section, non-linear problems are not a giant step up from the linear case.

In this example we consider the scenario where a factory is dumping pollutants into a river. We want to find out at what times and of what quantity it is doing this. It is not possible to get near the factory to directly measure this pollution inflow as a function of time, but we can place measurement devices downstream that measure pollution concentration (figure 2).

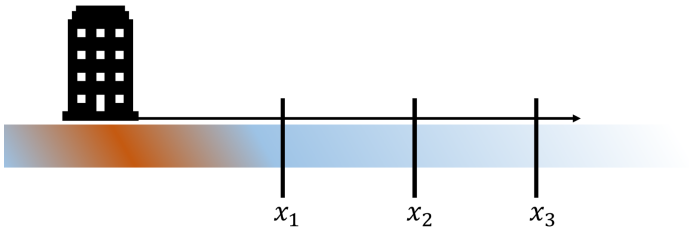

Figure 2: Source reconstruction problem. Given measurements downstream, we want to *reconstruct* the pollution inflow at the source as a function of time.

3.2 Mathematical Formulation

The diffusion equation is given by

$$\frac{\partial C}{\partial t} = D\frac{\partial^2 C}{\partial x^2} - v\frac{\partial C}{\partial x}$$

which has a solution in the form of a convolution

$$C(x,T) = \int_0^T g(x, T-t)C_{in}(t)dt \tag{3.1}$$

where

$$g(x,t) = \frac{x}{2\sqrt{\pi D t^3}} \exp\left(-\frac{(x-vt)^2}{4Dt}\right).$$

Equation (3.1) is the forward problem. $C(x,T)$ can be seen as our measurement data of pollution concentration downstream at a particular time T; g is the forward operator; and

C_{in} is the source pollution concentration as a function of time. Notice that the expression is linear in the term $C_{in}(t)$. This means we will be able to solve for $C_{in}(t)$ as a linear inverse problem. In the terminology of this example, finding $C_{in}(t)$ will be "reconstructing" the "source."

We can discretize 3.1 to obtain

$$d_i = C(x_i, T) \approx \sum_{j=1}^{n} g(x_i, T - t_j) C_{in}(t_j) \Delta t, \qquad i = 1, 2 \ldots, m.$$

where $\Delta t = T/n$. Letting $G_{ij} = g(x_i, T - t_j)\Delta t$ and $c_j = C_{in}(t_j)$, we get the matrix equation $d = Gc$, i.e.,

$$\begin{bmatrix} C(x_1,T) \\ C(x_2,T) \\ \vdots \\ C(x_m,T) \end{bmatrix} = \Delta t \begin{bmatrix} g(x_1,T-t_1) & g(x_1,T-t_2) & \cdots & g(x_1,T-t_n) \\ g(x_2,T-t_1) & g(x_2,T-t_2) & \cdots & g(x_2,T-t_n) \\ \vdots & \vdots & \ddots & \vdots \\ g(x_m,T-t_1) & g(x_m,T-t_2) & \cdots & g(x_m,T-t_n) \end{bmatrix} \begin{bmatrix} C_{in}(t_1) \\ C_{in}(t_2) \\ \vdots \\ C_{in}(t_n) \end{bmatrix}$$

We can solve for c using linear inverse problem theory. We set $n = 100$ and $m = 3$, meaning we have 3 measurements along the river and want to evaluate the source reconstruction to a resolution of 100 points. Notice that this is an underdetermined problem. Furthermore, we set $T = 300$, the diffusion coefficient as $D = 1$, and the flowrate as $v = 1$.

3.3 Modelling the Noise and Prior

Figure 3 shows the initial set of measurements. For the sake of the example, these measurements were taken from the true concentration shown in figure 3 with some normally distributed noise added. The noise added had a standard deviation of $\sigma_e = 0.1$, and assumes no correlation between data points (i.e. the off-diagonal entries in the covariance matrix will be zeros). In other words, the data covariance matrix is $\Gamma_e = \sigma_e^2 I$. In real-world situations it is important that the data standard deviation closely models how noisy the measurements are. If the standard deviation is too large, the measurements will have little influence on the posterior, hence the posterior will look like the prior; and if it is too small, the posterior will begin to be fit to the noise in the data, which is undesirable; furthermore, remember that in a real-world situation you will not have the true solution to compare to as we do here. Of course, it is also possible to model correlation of the noise between different data points by changing the off-diagonal entries of Γ_e.

Now, since we are working in the Bayesian framework, we have the benefit of using a prior. Recall that we will be using a normally distributed prior. Let's assume we have prior knowledge that the solution (i.e. the source reconstruction) is centered at value 3. Therefore

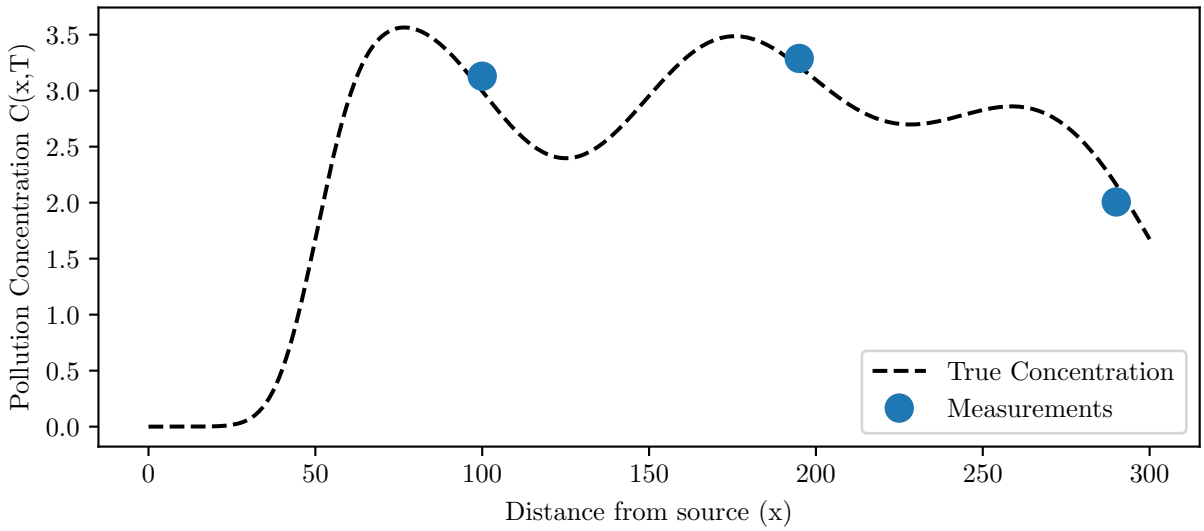

Figure 3: Pollution concentration at $T = 300$. The black dashed line shows the true underlying measurement model, and the blue dots show the measurements X_0 that were taken at $x = 100, 195, 290$. $x = 0$ is the source of the pollutant, i.e. the factory.

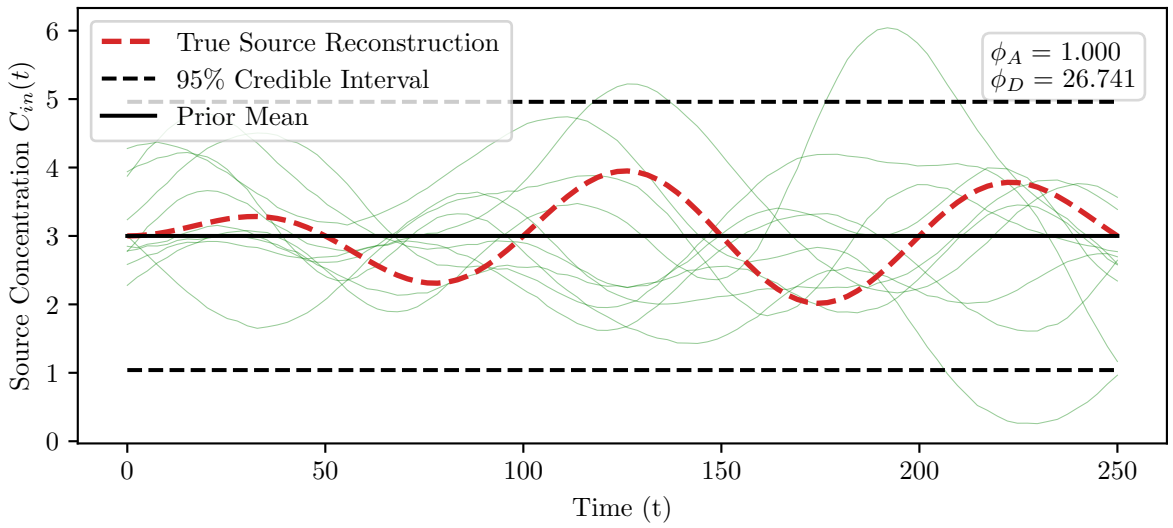

Figure 4: Prior source reconstruction distribution. The black line is the mean of the prior and the black dashed lines show the 95% credible interval of the normally distributed prior distribution. The red dashed line shows the true source concentration, which is what we want the posterior to hopefully be close to. The faint green lines are samples from the posterior distribution. The values in the box in the top right are evaluations of the uncertainty functions for the given measurement data.

we choose to use a constant function of value 3 as the prior mean. We set the prior standard deviation to be a constant $\sigma_c = 1$ for each parameter. In practical terms, what this means is that we are sure the solution lies somewhere in the range defined by this standard deviation around the value 3. This is shown in figure 4. Figure 4 shows the prior distribution with the solid black line being the prior mean μ_c. The faint green lines are samples taken from this distribution. It is always important to show some samples in a plot like this to see whether the distribution is doing what it is supposed to be doing. The values in the box in the top right of the plot are the uncertainty function values. These give a measure of the total uncertainty of the given measurement data (see figure 3 for the measurements), which, ideally, we are wanting to minimize. Note that we have modified the D-optimality function to be $\phi_D = 800 + \log(\det(\Gamma_{post}))$ in order to keep the values in a comparable range.

Notice that the true solution lies within the 95% credible interval. Though it might be difficult to know in advance how far the true solution will be from the prior, it is important to get this right. Similar to what was mentioned about the data covariance matrix, if we set the prior standard deviation to be too large, then the prior is essentially doing nothing; and if we set it to be too small, the posterior will look too much like the prior, that is, the constant function of value 3. This will be shown later. If in doubt, it might be better to set a slightly larger standard deviation. This will lead to more uncertainty in the posterior, but it is often better to be correct and uncertain than incorrect and certain. Note that a 95% credible interval simply shows the interval in which 95% of the probability lies. This is slightly different to a confidence interval, which is what we have in the frequentist framework. Figure 8 shows what happens when we set the prior standard deviation too small. This results in the true reconstruction lying outside of the credible interval. This is clearly undesirable. If we were to set the standard deviation too large, the opposite would occur: the credible interval would be too large.

We expect there to be correlations in concentration over time with nearby points; in other words, we expect the solution to be smooth; so we incorporate this into the prior covariance matrix Γ_c by using the squared exponential correlation function:

$$\{\Gamma_c\}_{ij} = \sigma_c^2 \exp\left(-\frac{(i-j)^2}{2L^2}\right) + \gamma I,$$

where we take the characteristic length scale $L = 10$, $\gamma = 10^{-4}$ to ensure positive definiteness, and I as the identity matrix. Figure 5 shows what Γ_c looks like as a heatmap. Notice how each parameter has exponentially diminishing correlation with its neighbouring parameters. Figure 7 shows what happens when we *do not use* the smoothness prior.

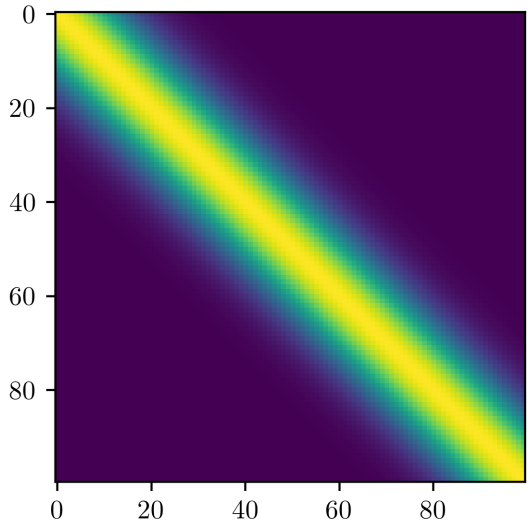

Figure 5: Prior covariance matrix Γ_c. This heatmap shows each parameter has exponentially diminishing correlation with its neighbouring parameters.

3.4 Computational Formulation

As seen in section 2.1.3, to evaluate the posterior, we set

$$A = \begin{bmatrix} L_e^{-1}G \\ L_c^{-1} \end{bmatrix}, \qquad b = \begin{bmatrix} L_e^{-1}d \\ L_c^{-1}\mu_c \end{bmatrix}$$

where L_e and L_c come from the Cholesky decompositions (which can be found using a function in most numerical packages), i.e., $\Gamma_e = L_e^T L_e$ and $\Gamma_c = L_c^T L_c$. Furthermore, μ_c is the prior mean, which we said represents the constant function of value 3. Here this means μ_c is a vector of 3's. To evaluate the posterior mean and covariance we use

$$c_{MAP} = (A^T A)^{-1} A^T b \quad \text{and} \quad \Gamma_{post} = (G^T \Gamma_e^{-1} G + \Gamma_c^{-1})^{-1}.$$

We can then use these to sample from the normally distributed posterior. Figure 6 shows the posterior distribution of the source reconstruction. This plot is similar to the prior distribution plot (figure 4). This posterior is not of primary interest in this paper, but is used as a *reference posterior* to which we compare other posteriors that have measurements added. Notice that the mean of the distribution does not line up very well with the true reconstruction, and that the credible interval is quite large in certain areas. This means that we need to either a) add more measurements, b) take measurements that contain less error, or c) use a better prior containing more information. In what follows we take the first approach in adding more measurements.

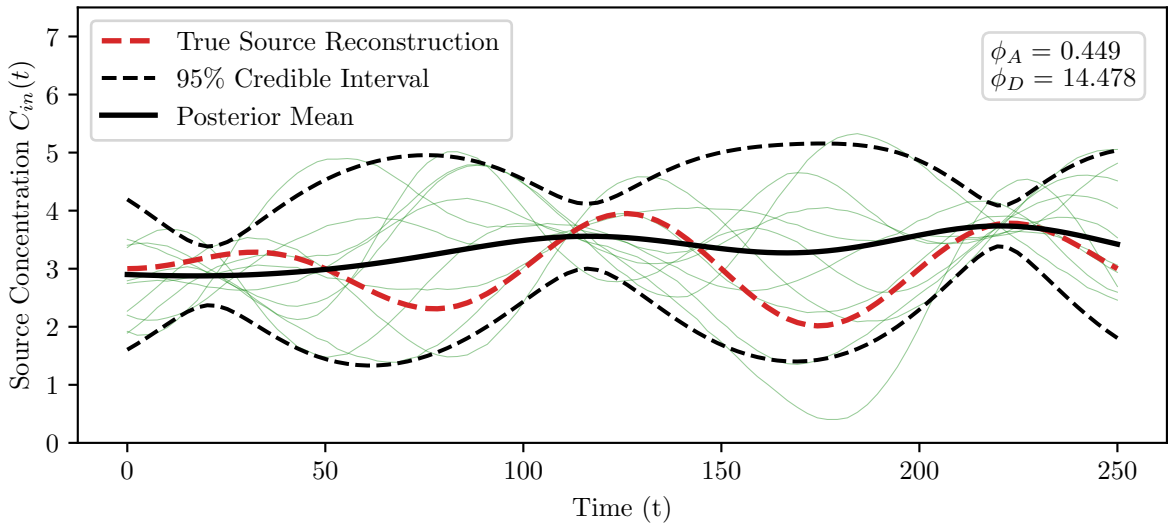

Figure 6: Posterior source reconstruction distribution for the measurements X_0. Notice that the uncertainty function values in the upper right box are reduced from the prior distribution plot (figure 4).

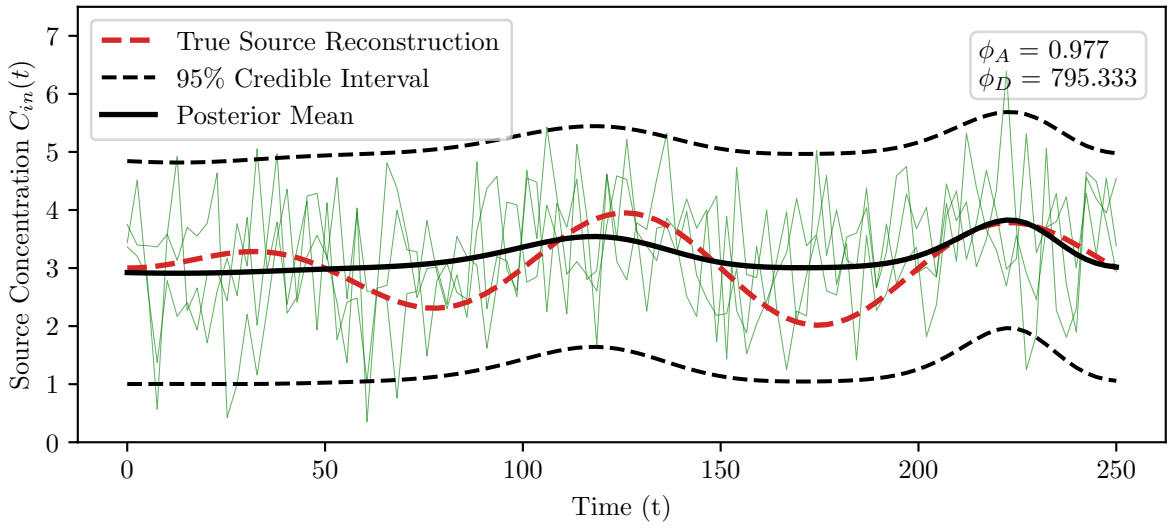

Figure 7: This plot shows what happens when you do not use the smoothness prior. The samples become a lot more jagged. Here the number of samples has been reduced to 3, to show what is happening. In this case the prior covariance matrix has simply been set as $\Gamma_c = \sigma_c^2 I$.

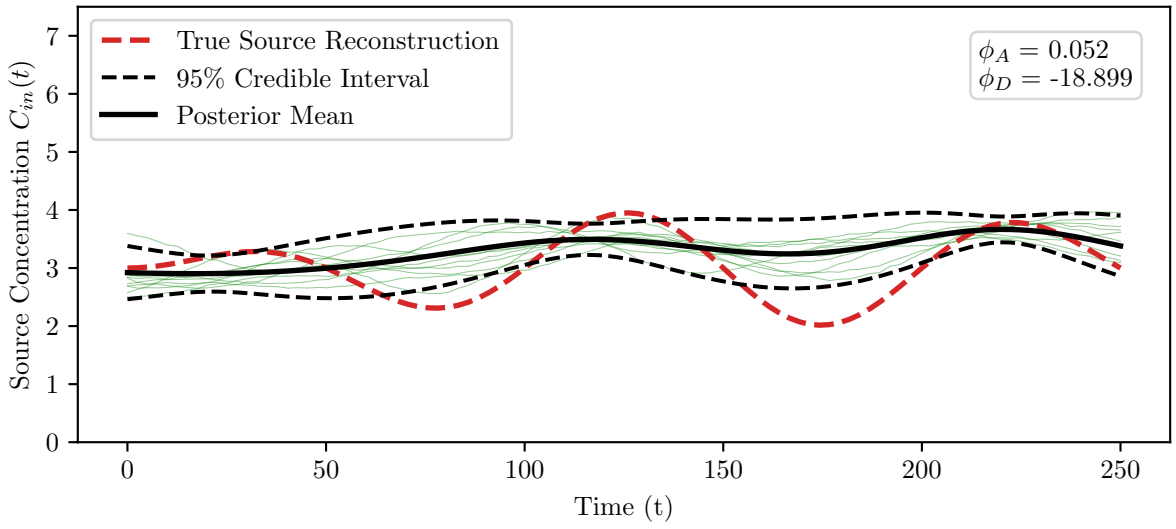

Figure 8: Prior variance set too small. Notice the true reconstruction lies outside the credible interval.

3.5 Adding Measurements

In this section we assume that the cost of taking measurements is the same everywhere, hence for the time being we do away with the cost penalty term $P(x)$. We add the set of five measurements $X_{new}^{(1)}$ shown in figure 9. The reason we add a set of measurements here instead of one new measurement is just for the sake of example, because the change in measurement uncertainty in the posterior will be more noticeable. Figure 10 shows the posterior for the measurement set $X_0 \cup X_{new}^{(1)}$. Notice that the uncertainty is significantly reduced on the right. Furthermore, the mean is better fit in this region. Notice also that the uncertainty function values are significantly reduced as compared with the posterior of the measurement set X_0 (figure 6). Figure 11 show a different additional measurement set $X_{new}^{(2)}$. The posterior associated with $X_0 \cup X_{new}^2$ is shown in figure 12. Figure 13 shows the posterior for both sets of additional measurements, that is, $X_0 \cup X_{new}^{(1)} \cup X_{new}^{(2)}$.

From the figures referred to above, it is clear that adding measurements at certain locations results in the posterior having reduced uncertainty in other specific locations. As long as the measurements we use are reasonably good, adding more will almost always result in uncertainty reduction somewhere. When looking at figures 10 and 12, it might be asked why adding measurements on one side of the space-domain produces uncertainty reduction on the opposite side of the time domain. Considering figures 11 and 12 as an example, although unclear at first, it seems the reason for this opposite-end uncertainty reduction is due to the relationship between the time periods associated with the two plots. Figure 11 gives a

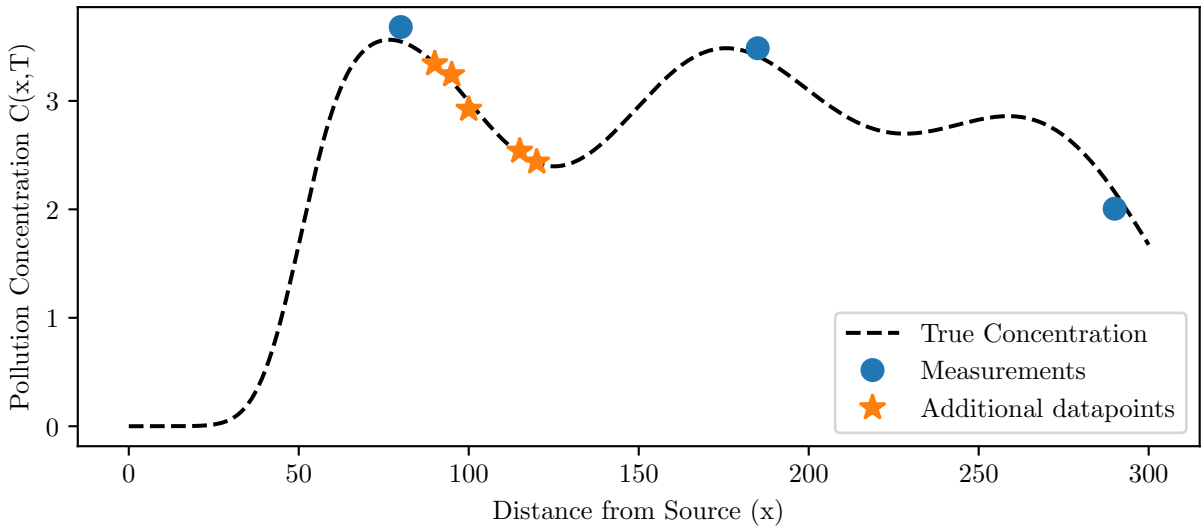

Figure 9: Additional measurements 1. The five orange stars make up the additional measurement set $X_{new}^{(1)}$.

snapshot in time at $T = 300$, and the measurements added on the far right measure the pollution concentration produced at the factory at the beginning of the time cycle, that is, the left side of figure 12.

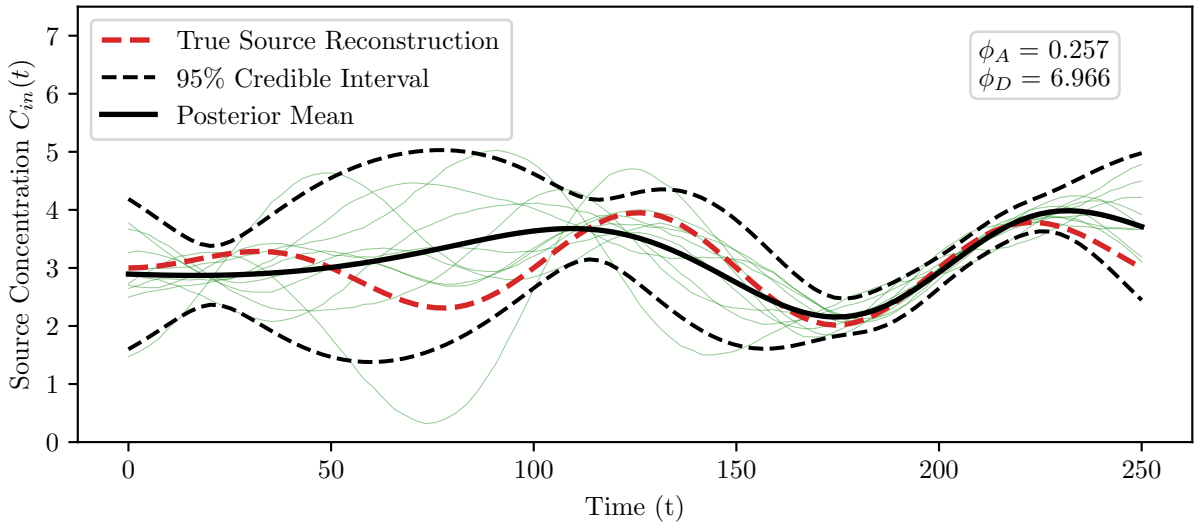

Figure 10: The posterior distribution that belongs to the measurement set $X_0 \cup X_{new}^{(1)}$.

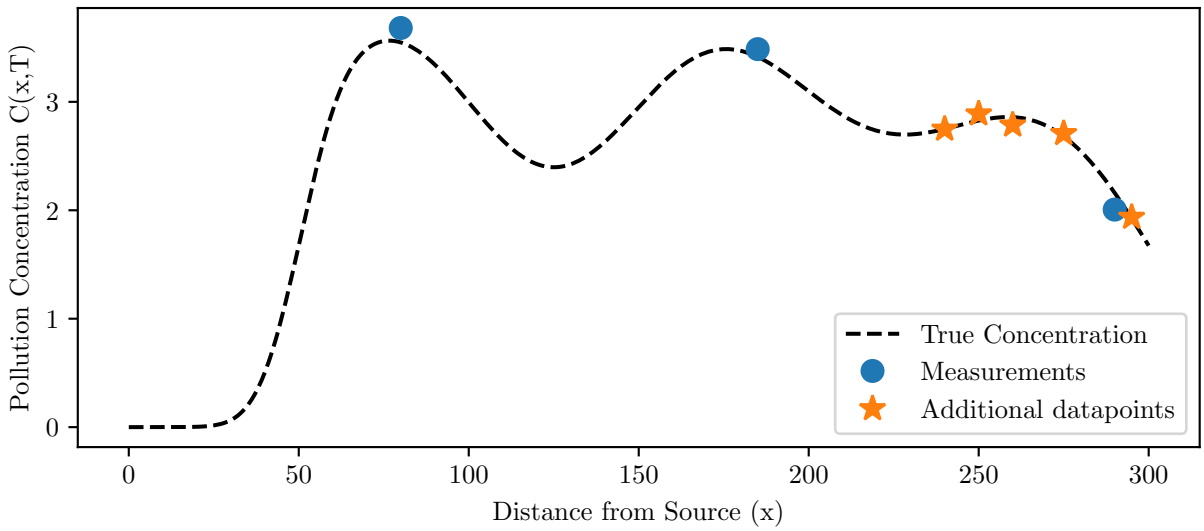

Figure 11: Additional measurements 1. The five orange stars make up the additional measurement set $X_{new}^{(2)}$.

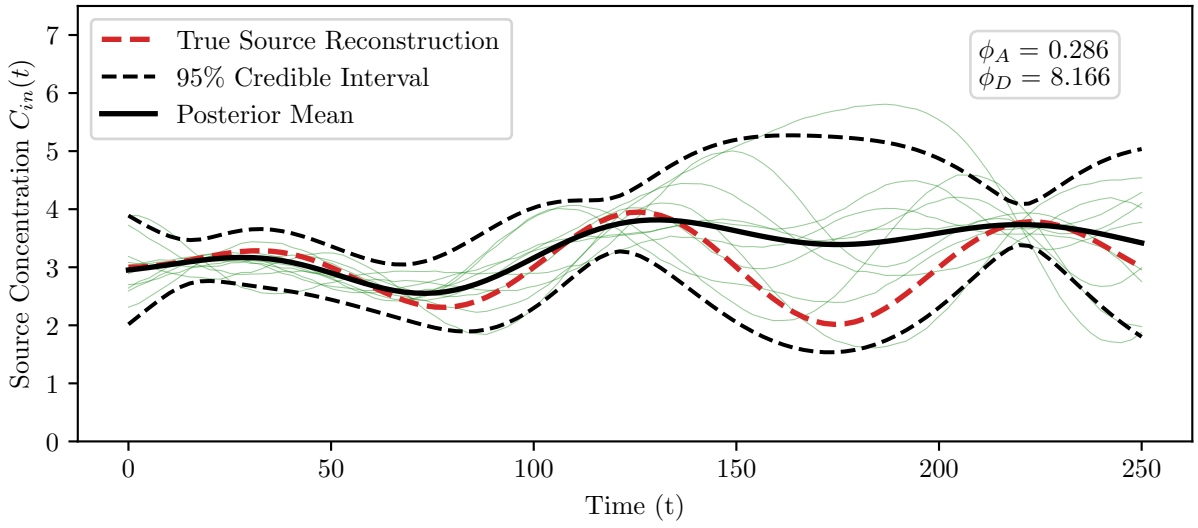

Figure 12: The posterior distribution that belongs to the measurement set $X_0 \cup X_{new}^{(2)}$.

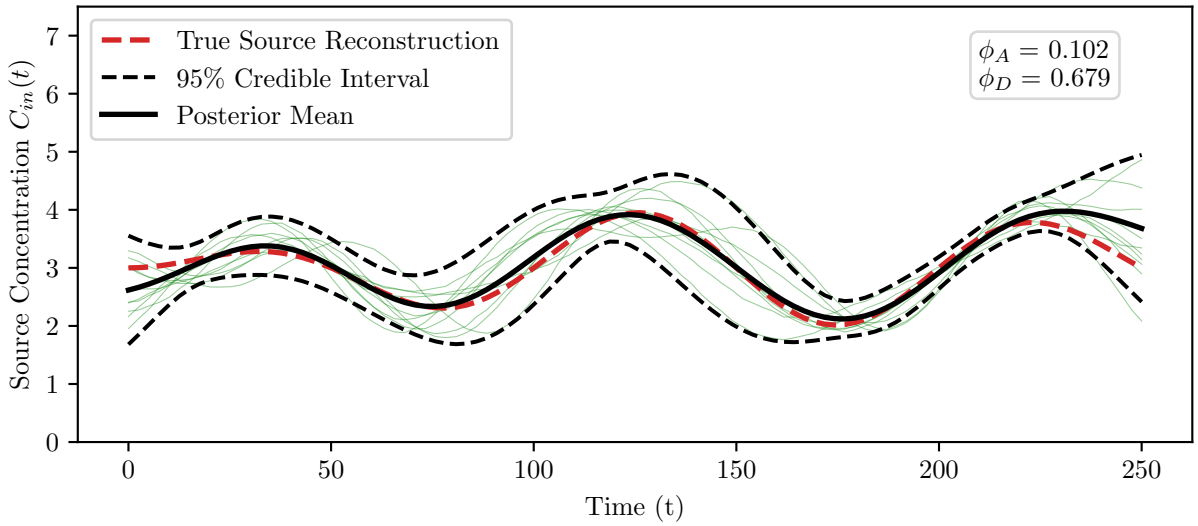

Figure 13: The posterior distribution that belongs to the measurement set $X_0 \cup X_{new}^{(1)} \cup X_{new}^{(2)}$.

3.6 Dual Objective Data-Worth Analysis

Until now we have looked at what it means to minimize posterior uncertainty without regard for the cost function. But now we turn our attention again to the total objective, the task of minimizing both uncertainty and cost simultaneously:

$$\min_{X \in \mathcal{M}} \phi_I(\Gamma_{post}^{(X)}) + P(X), \quad I \in \{A, D\}.$$

Figure 14 shows our setup. We again have the same 3 initial measurements as before, X_0, but now we also have a linear cost function. This function is set so that cost decreases as we move further away from the pollution source. The dotted line also sets a boundary to the left of which we are unable to gather measurements. Another way to view this region is as a region having infinite cost. Note that we continue from hereon using only the A-optimality uncertainty function.

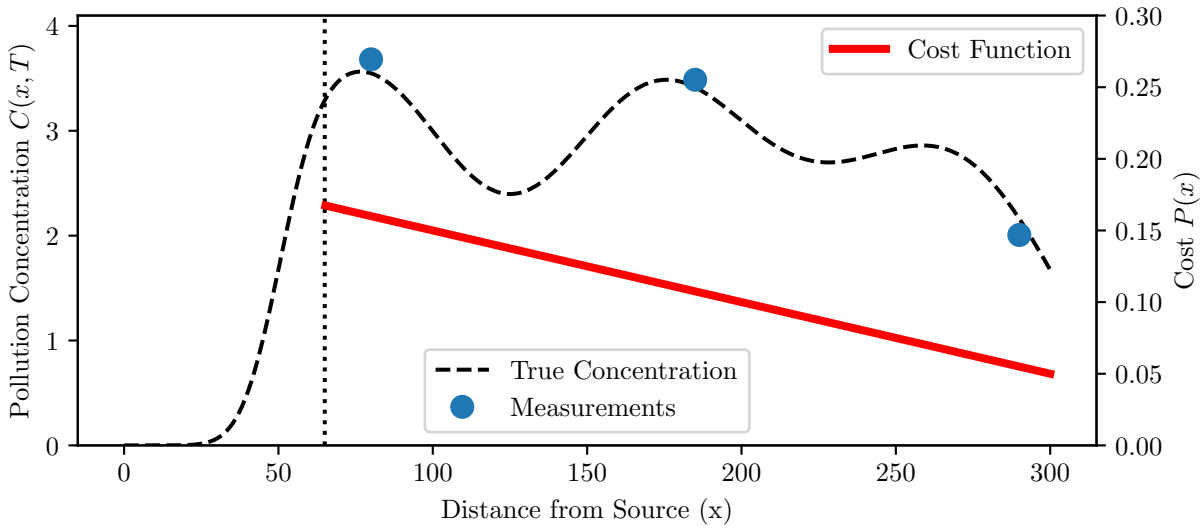

Figure 14: The same initial set up of the intial measurements X_0 as before. But we know utilize the linear cost function shown in red.

Figure 15 shows the decomposition of the objective function. The main function of interest is the black line, which is the composition $\phi_A + P(x)$. The orange dashed line is the uncertainty function on its own. It is evaluated all along the x-axis; in other words, at each (discrete) point along the x-axis, the posterior is evaluated, and the uncertainty objective value is computed to show us how the uncertainty would change if we were to add a measurement at that location. The vertical dashed line, indicating $x_{optimal}$, shows where the next optimal measurement location is for the given domain. Figure 15 shows the first iteration. In this

case $x_{optimal}$ is chosen where the orange dashed line, ϕ_A, is minimized. In reality we actually want to be minimizing the black line, $\phi_A + P(x)$, but we start here to illustrate a point.

Figure 16 shows the iterative process. At each iteration the minimizer of the orange dashed line is accepted as the new measurement location to be added, i.e., we iteratively add $X_0 \cup X^1_{new} \cup X^2_{new} \cdots \cup X^N_{new}$. We call this the *greedy* approach. The plot on the bottom right, which skips ahead to iteration 18, shows that in our current set up of minimizing the orange line, we eventually minimize uncertainty as low as it can go. This is shown again in figure 18 where we see what happens as we add more and more measurement locations. The black dashed line shows how the uncertainty of the greedy method minimizes and eventually flattens out. The orange dashed line shows a *random* approach where instead choosing the optimal measurement location at each iteration, a random location is chosen. Clearly, the greedy method beats this random approach. However, they both converge eventually. Because the cost objective is not considered in the current objective scheme, the discrepancy between the random and greedy costs (solid black and orange) can be considered to be purely due to random chance.

Consider now the real case where we use the total objective $\phi_A + P(x)$. The iterations are shown in figure 17. In this case we are minimizing the black function, and we see that uncertainty does not necessarily reduce all the way because the cost function now plays a role in choosing the next measurement location. Because of this, as we see in figure 19, the black line (greedy method) plateaus, but the random method actually dips below it and eventually ends up giving us a better result. The bottom right plot of figure 17 gives us hint at why this is: it seems the algorithm gets stuck at the low point of the total objective.

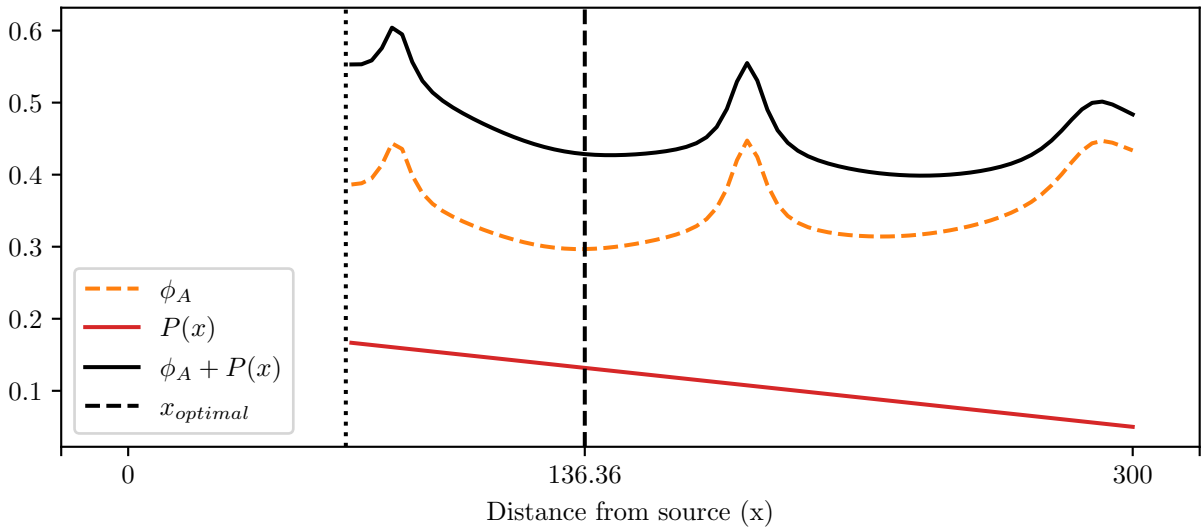

Figure 15: Decomposition of the total objective function. The vertical black dotted line shows the threshold of the region where we are not allowed to take measurements. The vertical black dashed line shows the next optimal measurement location. The orange dashed line shows the uncertainty function evaluated at different measurement locations. The red line shows the cost function. And the solid black line shows the total objective function.

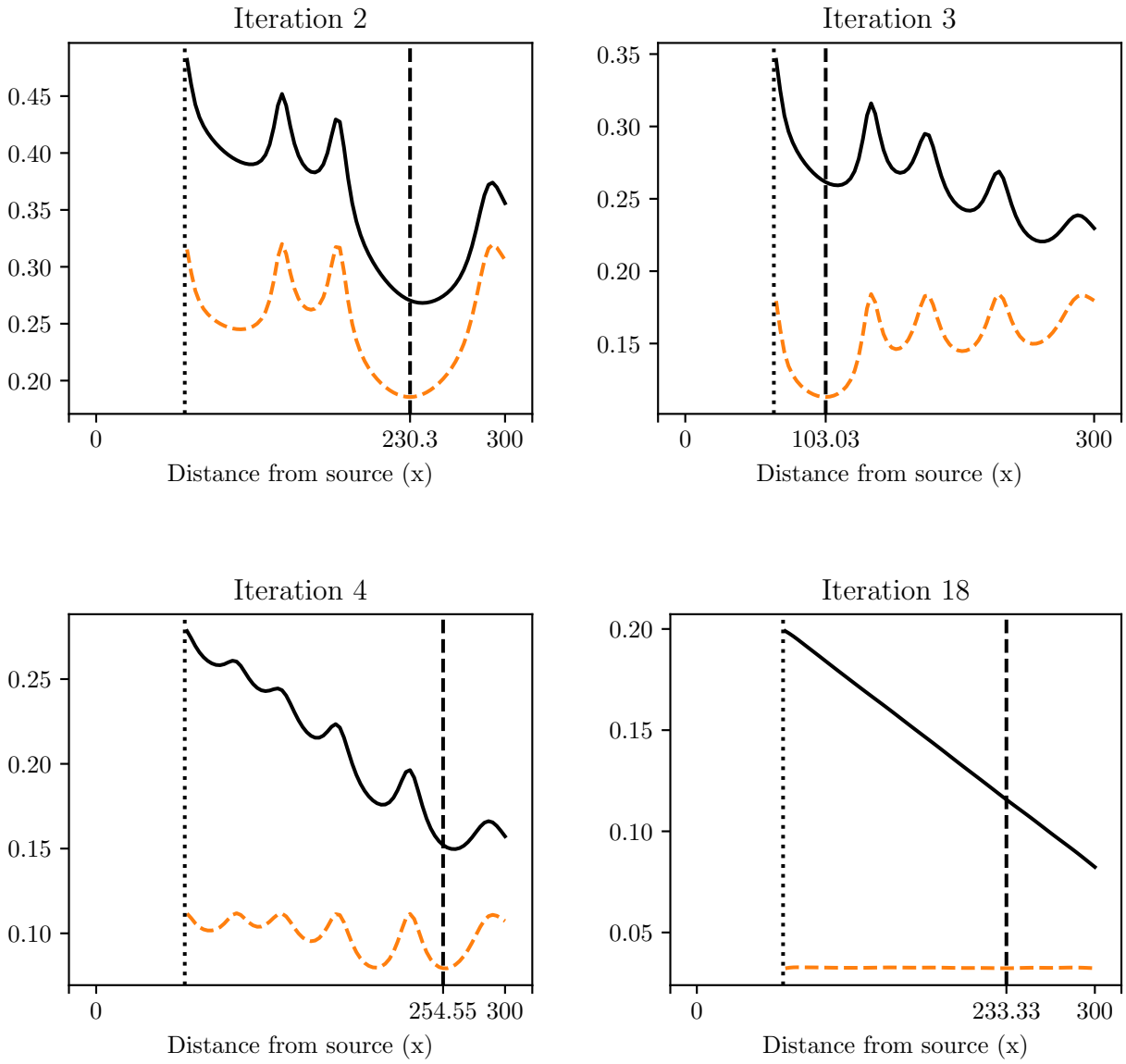

Figure 16: Iterative procedure showing $x_{optimal}$ being chosen at each step. Here $x_{optimal}$ is chosen such that the orange line is minimized. Refer to figure 15 for the meanings of the different lines.

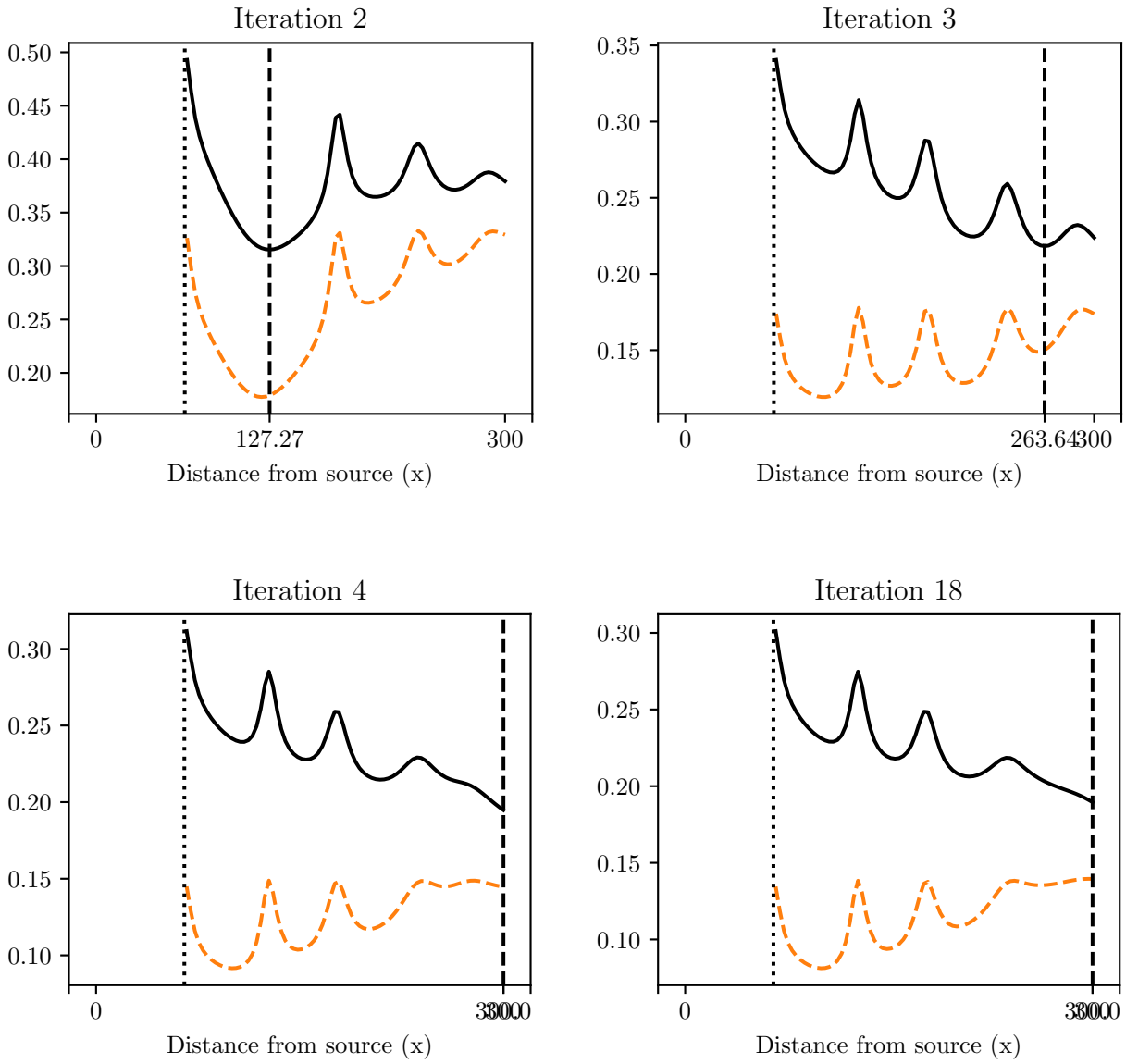

Figure 17: Iterative procedure showing $x_{optimal}$ being chosen at each step. Here $x_{optimal}$ is chosen such that the black line is minimized. Refer to figure 15 for the meanings of the different lines.

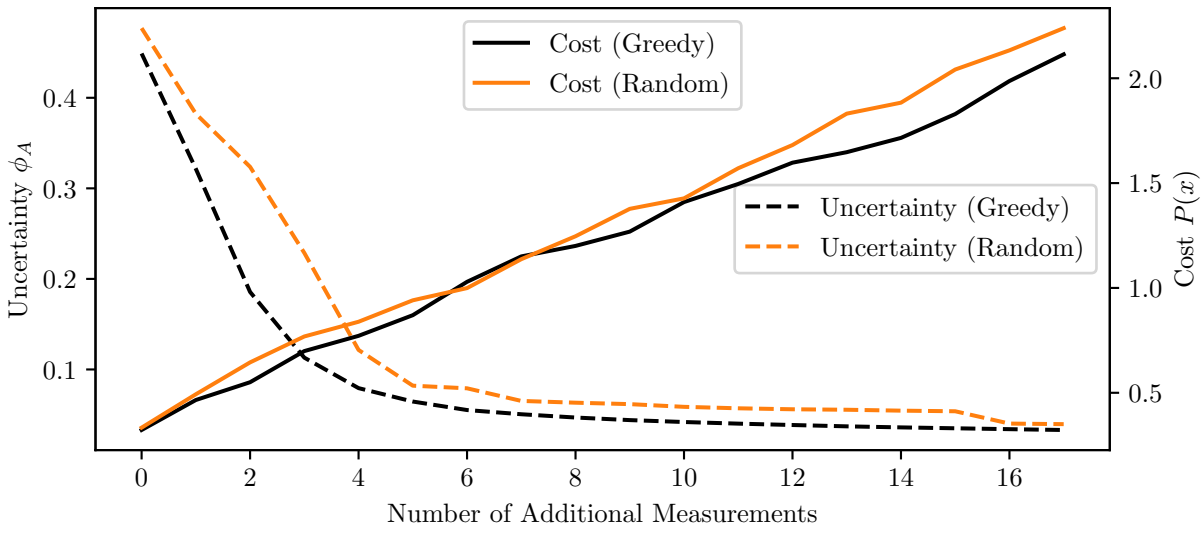

Figure 18: Uncertainty and cost as a function of iteration count. This plot shows the case where we are minimizing ϕ_A only.

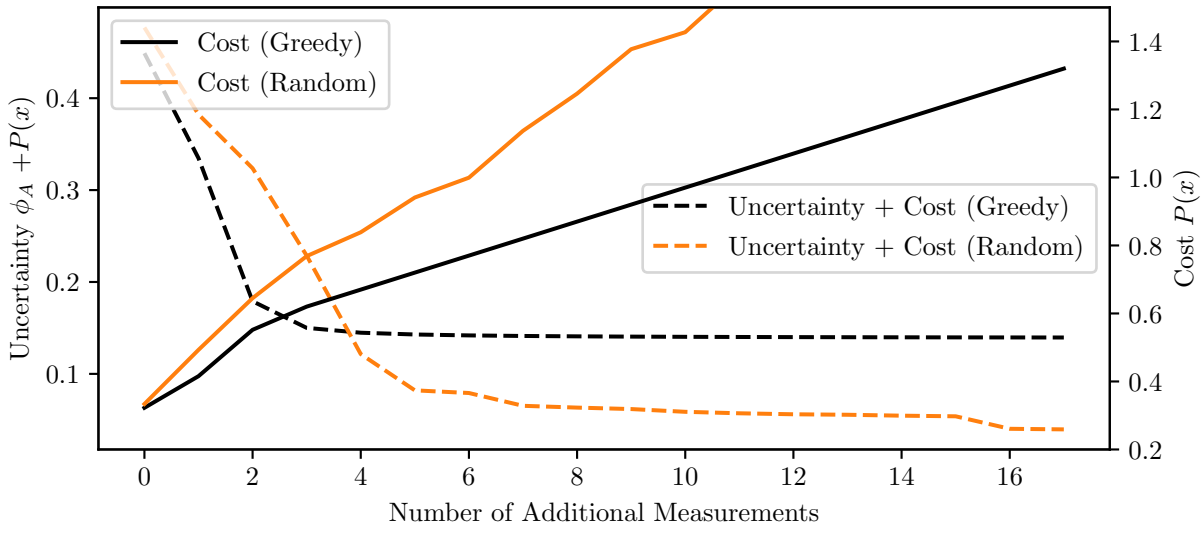

Figure 19: Uncertainty and cost as a function of iteration count. This plot shows the more appropriate case where we are minimizing $\phi_A + P(x)$, i.e., where the cost of the measurement location is now also considered.

Bibliography

[1] R. Nicholson, H. Alferink, E. Paton-Simpson, O. J. Maclaren, *et al.*, "An introduction to optimal data collection for geophysical model calibration problems," *New Zealand Geothermal Workshop*, 2020.

[2] J. Kaipio and E. Somersalo, *Statistical and computational inverse problems (Vol. 160).* Society for Industrial and Applied Mathematics, 2006.

[3] A. Tarantola, *Inverse problem theory and methods for model parameter estimation.* Society for Industrial and Applied Mathematics, 2005.

[4] A. Alexanderian, "Optimal experimental design for bayesian inverse problems governed by pdes: A review," *arXiv preprint arXiv:2005.12998*, 2020.

[5] S. Finsterle, "Practical notes on local data-worth analysis," *Water Resources Research, 51(12)*, pp. 9904–9924, 2015.

[6] R. C. Aster, B. Borchers, and C. H. Thurbur, *Parameter Estimation and Inverse Problems.* 2013.